Supporting Information

Barrera et al. 10.1073/pnas.1212665109

SI Text

SI Materials and Methods. ***pHLIP peptides.*** All peptides were prepared by standard solid phase synthesis using 9-fluorenylmethyloxycarbonyl chemistry at the W.M. Keck Foundation Biotechnology Resource at Yale University and purified by reverse phase chromatography. Purity was checked by MALDI-TOF mass spectrometry. All peptides were quantified by absorbance spectroscopy, using a molar extinction coefficient of 13,940 M^{-1} cm^{-1}. The sequences of the employed peptides, with the cysteine residues employed for dye labeling underlined, were:

WT pHLIP: GGEQNPIYWARYADWLFTTPLLLLDLALLV DADEGTCG

ACEQNPIYWARYADWLFTTPLLLLDLALLVDADEGTG

P20G: AAEQNPIYWARYADWLFTTGLLLLDLALLVDAD EGT

ACEQNPIYWARYADWLFTTGLLLLDLALLVDADEGT

To rule out the possibility that intermolecular disulfide bonds might be occurring we ran HPLC of the pHLIP peptide. No peptide dimer was observed after 3 h incubation at 10 μM peptide in the presence or in the absence of liposomes. Only under extreme conditions (overnight incubation at 100 μM peptide) did we observe small amounts of dimer (approximately 10%).

Analytical ultracentrifugation. Sedimentation velocity experiments were performed at 20 °C with a Beckman An-60Ti rotor in a Beckman Optima XL-I ultracentrifuge at 98,784 g (35.000 rpm). Peptide was dissolved in 5 mM phosphate buffer, pH 8, at 7 μM and incubated for 1 h at room temperature. Sedimentation was followed by absorbance at 280 nm, and the continuous sedimentation coefficient distribution was obtained using SEDFIT (1). The following parameters were employed for the continuous c(s) distribution analysis: Frictional ratio of 1.3, partial specific volume of 0.73 cm^3/g, buffer density of 0.99590 g/mL and buffer viscosity of 0.00893 Poise.

Liposome preparation. All lipids were purchased from Avanti Polar Lipids (biological source/molecular names and catalogue number are provided): Cholesterol (ovine wool, 700,000P), 14:1-PC (1,2-dimyristoleoyl-sn-glycero-3-phosphocholine, 850,346C), 16:1-PC (1,2-dipalmitoleoyl-sn-glycero-3-phosphocholine, 850,358C), 18:1-PC (1,2-dioleoyl-sn-glycero-3-phosphocholine, 850,375C), 20:1-PC (1,2-dieicosenoyl-sn-glycero-3-phosphocholine, 850,396C) and 22:1-PC (1,2-dierucoyl-sn-glycero-3-phosphocholine, 850,398C). A liver total lipid extract (bovine, 181,104C) was also employed, containing (wt/wt%) 42% PC, 22% PE, 8% PI, 1% lyso-PI, 7% cholesterol and 21% others, including neutral lipids. The required volume of a 25 mg/mL chloroform-dissolved lipid stock was placed in a glass tube and dried with argon before overnight drying under vacuum. Dried films were resuspended in 50 mM phosphate buffer (pH 7) for cholesterol-containing experiments and 5 mM phosphate buffer (pH 8) for vesicles not containing cholesterol. This strategy was used because a lower solution ionic strength gave irregularities in the state II peptide partitioning to membranes containing cholesterol. In both cases, the resuspended lipids were vortexed to a final concentration between of 4–10 mM. Extrusion was performed using a Mini-Extruder (Avanti Polar Lipids), with Nuclepore polycarbonate membranes of 0.1 μm pore size (Whatman). To obtain the final large unilamellar vesicles (LUVs), repeated extrusion steps were performed until the turbidity of the solution could not be further decreased (15–60 steps depending on the lipid type and concentration, typically resulting in a very transparent suspension). Extrusion was performed at room temperature for all lipids except the liver total extract, where the Mini-Extruder block was heated to 50 °C.

Fluorescence determination of pKa. Peptides were dissolved in 5 mM phosphate buffer, pH 8, and incubated with lipid vesicles prepared in the same buffer as above, resulting in molar lipid to peptide ratios of 250:1 or 300:1. The pH of individual samples was adjusted with appropriate 100 mM stock buffers for the following pH ranges: Sodium acetate, pH 3.5–5.5 and Na_2HPO_4/NaH_2PO_4, pH 5.5–8.0. The final peptide concentration was 1.5 μM and the final solution ionic strength was 28 mM for experiments containing cholesterol and 15 mM for all others (see above). Emission spectra were measured on a SLM-Aminco 8,000C spectrofluorimeter at 25 °C with excitation at 295 nm. The appropriate blanks were subtracted in all cases. For the determination of spectral maxima we used the FCAT mode of the PFAST software, which fits the experimental spectra to log-normal components (2, 3). The wavelength of maximum emission thus obtained for each sample of the pH curve were plotted, and analyzed according to (4):

$$F = \frac{(F_a + F_b 10^{m(\mathrm{pH}-pK\mathrm{a})})}{(1 + 10^{m(\mathrm{pH}-pK\mathrm{a})})}, \qquad \textbf{[S1]}$$

where $F_a = (f_A + S_A\ \mathrm{pH})$ and $F_b = (f_B + S_B\ \mathrm{pH})$; f_A and f_B are the spectral maxima for the acid and basic forms, respectively, S_A and S_B are the slopes of the acid and base baselines, and m is the cooperativity parameter. Alternatively, the monitoring of fluorescence intensity might yield a more representative pKa value (5); however, after careful examination of different fluorescence parameter analysis, we found that the specific parameter used to obtain pKa does not affect the conclusions of the paper. Fitting by nonlinear least squares analysis was carried out with Origin (OriginLab, MA).

Circular dichroism. Peptides were dissolved in 5 mM phosphate buffer (pH 8) to an initial concentration of approximately 30 μM. This peptide solution was then diluted with LUVs solution in the same buffer to a final peptide concentration of 10 μM. The resulting stock had a molar lipid to peptide ratio of 200:1 or 300:1. This stock solution was incubated for 1 h before use. The pH of individual samples was adjusted with 100 mM stock buffers. After adjustment, the final peptide concentration was 5 μM and the final solution iconic strength was 28 mM for experiments containing cholesterol and 15 mM for all others. Spectra were recorded in a Jasco J-810 circular dichroism spectropolarimeter interfaced with a Peltier system. A 2 mm pathlength quartz cuvette was employed. Spectra were recorded at 25 °C with 100 nm/min scan rate and 10–50 averaging steps. Raw data was converted to mean residue ellipticity according to (6):

$$[\Theta] = \Theta/(10\ \boldsymbol{lcN}), \qquad \textbf{[S2]}$$

where Θ is the measured ellipticity, $\boldsymbol{l}$ is the pathlength of the cell, $\boldsymbol{c}$ is the protein concentration, and $\boldsymbol{N}$ is the number of amino acids. For the study of membrane attachment and insertion, the typical procedure was as follows: Samples were incubated with LUVs at pH 8 for 60 min and spectra recorded; then the pH was lowered to 4.0 and after 30 min measurements were performed. Appropriate blanks were subtracted in all cases.

Cell culture. B104 and COS-7 cell lines were a kind gift from Maureen Gilmore-Hebert and David F. Stern (Yale University). B104 is a rat neuroblastoma cell line (7), and COS-7 is an African green monkey kidney fibroblast-like cell line (8). Cells were cultured in DMEM supplemented with 4.5 g/L D-glucose and L-glutamine, 10% FBS and penicillin/streptomycin (10.000 units/10.000 μg; 100×). Cells were grown in an incubator under a humidified atmosphere of air and 5% CO_2 at 37 °C.

Plate reader determination of peptide insertion in cultured cells. WT pHLIP and P20G were labeled covalently at the N-terminal cysteine with Alexa Fluor 594 C_5-maleimide. Peptide and dye reagent were resuspended in 5 mM Pi buffer, pH 7.5, and the reaction was carried out for 2 h at room temperature (under agitation and protected from light). The product from the reaction was separated from the free dye using a Sephadex G25 M column. The assay was performed with 2.2 μM of the labeled peptides, resuspended in Dulbecco's Phosphate Buffered Saline (DPBS) supplemented with Ca^{2+} and Mg^{2+} and 10 mM dextrose. Quantification was carried out by employing the absorbance of the Alexa dye ($\varepsilon = 73.000\ M^{-1}\ cm^{-1}$). Cells were grown on UV-sterilized collagen-coated 96-well plates (NUNC), to 90–95% confluency (approximately 50.000 cells). After three rinses with Dulbecco's Phosphate Buffered Saline (DPBS), the peptide was incubated for 2 min and then DPBS supplemented with 20 mM of additional buffering agent was added to reach different final pHs: Citric acid (final pH 4.5–5.5), MES (pH 5.5–7.1) or Hepes (pH 7.0–8.0). After 1 min, the solution was removed to measure the final pH. Three DPBS rinses of the cells were performed and the fluorescence was measured in a PTI FluoDia T70 plate reader, with 560 nm excitation filter and 620 nm emission filter. Cell viability was determined in the same 96-well plate used for the fluorescence measurement by adding a small aliquot of cell titer 96 AQueous One solution cell proliferation assay (Promega). Absorbance was measured on a Berthold TriStar LB941 plate reader, with a 490 nm filter.

Plasma membrane cholesterol depletion. Methyl-β-cyclodextrin (MβCD) was employed to remove cholesterol from cultured cells. Cells were washed with DMEM, and incubated for 1 h with 5 mM M β CD dissolved in DMEM supplemented with 25 mM Hepes, pH 7.4. The extent of cholesterol removal was determined as in ref. 9. Briefly, treated and control cells were scrapped, and the plasma membrane fraction separated in a discontinuous sucrose gradient. Total lipids were extracted (10), quantified (11) and the cholesterol content was determined using an enzymatic fluorescent assay (Amplex Red, Invitrogen).

DPH anisotropy. The fluorescence probe diphenylhexatriene (DPH) was dissolved in methanol to make an 80 μM concentrated stock. A small DPH aliquot (0.2% mol of the lipid) was added to samples containing 0.45 mM of the different LUVs, and after 2–3 h incubation the anisotropy of the DPH was measured ($\lambda_{ex} = 358$ nm, $\lambda_{em} = 430$ nm). For experiments in cell membrane fractions, the sucrose of the solution was removed by dialysis, and the experiment was performed as in the LUV experiments.

Cell translocation assay. pHLIP was labeled at the C-terminal cysteine residue with TS-Link BODIPY 630/650 C_5-thiosulfate, sodium salt ($\varepsilon = 101.000\ M^{-1}\ cm^{-1}$), resulting in a disulfide bond which can be cleaved by the reducing conditions present in the cytosol. Cells were grown in glass bottom dishes (Electron Microscopy Sciences) and live cell confocal microscopy was performed on a Zeiss LSM 510 NLO META using a 20× objective (12). Peptide concentration was 3 μM, and cells were treated with the peptide using the same conditions as the plate reader assay, with the exception that the final washing solution contained 10% FBS.

1. Schuck P (2000) Size-distribution analysis of macromolecules by sedimentation velocity ultracentrifugation and lamm equation modeling. *Biophys J* 78:1606–1619.
2. Burstein EA, Abornev SM, Reshetnyak YK (2001) Decomposition of protein tryptophan fluorescence spectra into log-normal components. I. Decomposition algorithms. *Biophys J* 81:1699–1709.
3. Shen C, et al. (2008) The protein fluorescence and structural toolkit: Database and programs for the analysis of protein fluorescence and structural data. *Proteins* 71:1744–1754.
4. Ionescu RM, Eftink MR (1997) Global analysis of the acid-induced and urea-induced unfolding of staphylococcal nuclease and two of its variants. *Biochemistry* 36:1129–1140.
5. Moon CP, Fleming KG (2011) Using tryptophan fluorescence to measure the stability of membrane proteins folded in liposomes. *Methods Enzymol*. 492:189–211.
6. Kelly SM, Price N (2000) The use of Circular Dichroism in the investigation of protein structure and function. *Current Protein Pept Lett* 1:349–384.
7. Schubert D, et al. (1974) Clonal cell lines from the rat central nervous system. *Nature* 249:224–227.
8. Gluzman Y (1981) SV40-transformed simian cells support the replication of early SV40 mutants. *Cell* 23:175–182.
9. Mitra K, Ubarretxena-Belandia I, Taguchi T, Warren G, Engelman DM (2004) Modulation of the bilayer thickness of exocytic pathway membranes by membrane proteins rather than cholesterol. *Proc Natl Acad Sci USA* 101:4083–4088.
10. Bligh EG, Dyer WJ (1959) A rapid method of total lipid extraction and purification. *Can J Biochem Physiol* 37:911–917.
11. Stewart JC (1980) Colorimetric determination of phospholipids with ammonium ferrothiocyanate. *Anal Biochem* 104:10–14.
12. Thevenin D, An M, Engelman DM (2009) pHLIP-mediated translocation of membrane-impermeable molecules into cells. *Chem.Biol* 16:754–762.

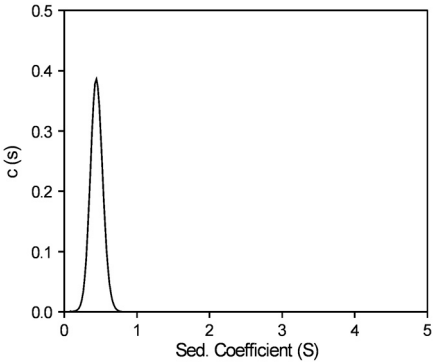

Fig. S1. Analytical ultracentrifugation of P20G in solution. The apparent sedimentation coefficient distribution is shown, as derived from sedimentation velocity profile of the peptide in 5 mM phosphate buffer, pH 7.8, at 7 μM. A single population is seen, with an S of 0.61 ± 0.24, corresponding to a molecular weight of 2.6 ± 1.9 KDa (expected monomer molecular weight = 4039.6 Da).

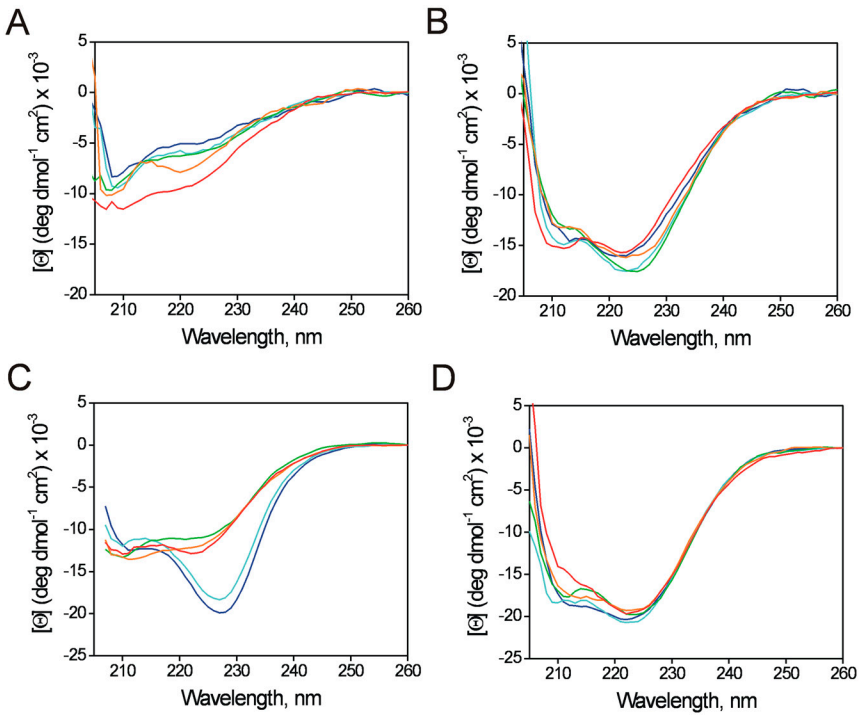

Fig. S2. Circular dichroism (CD) spectra of P20G and WT pHLIP for states II and III. (*A*) CD spectra of pHLIP in different liposomes at pH 7.8 (state II). (*B*) CD of pHLIP in liposomes at pH 4.5 (state III). (*C*) CD of P20G in liposomes at pH 7.8 (state II). (*D*) CD of P20G in liposomes at pH 4.5 (state III). The different liposomes employed were: 14:1-PC (blue), 16:1-PC (cyan), 18:1-PC (green), 20:1-PC (orange) and 22:1-PC (red). Different scales were used in boxes *A*–*B* and *C*–*D*.

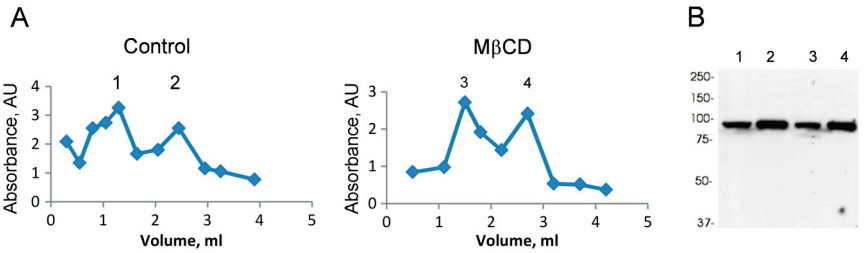

Fig. S3. Sucrose gradient separation of membrane fractions. (*A*) Control and MβCD-treated cells were disrupted and loaded in a sucrose gradient. The absorbance at 280 nm of the collected fractions was measured, and two peaks, corresponding to different membrane fractions, were detected in both conditions (labeled 1–4). (*B*) An aliquot of each peak sample was loaded in a western blot detecting the alpha subunit of the Na^+/K^+-ATPase, a protein enriched in the plasma membrane. Despite lower membrane content in fractions 2 and 4, more intense bands were obtained, indicating that these fractions are enriched in plasma membrane, while fractions 1 and 3 are enriched in microsomal membranes. Protein markers are shown in the gel, in KDa.

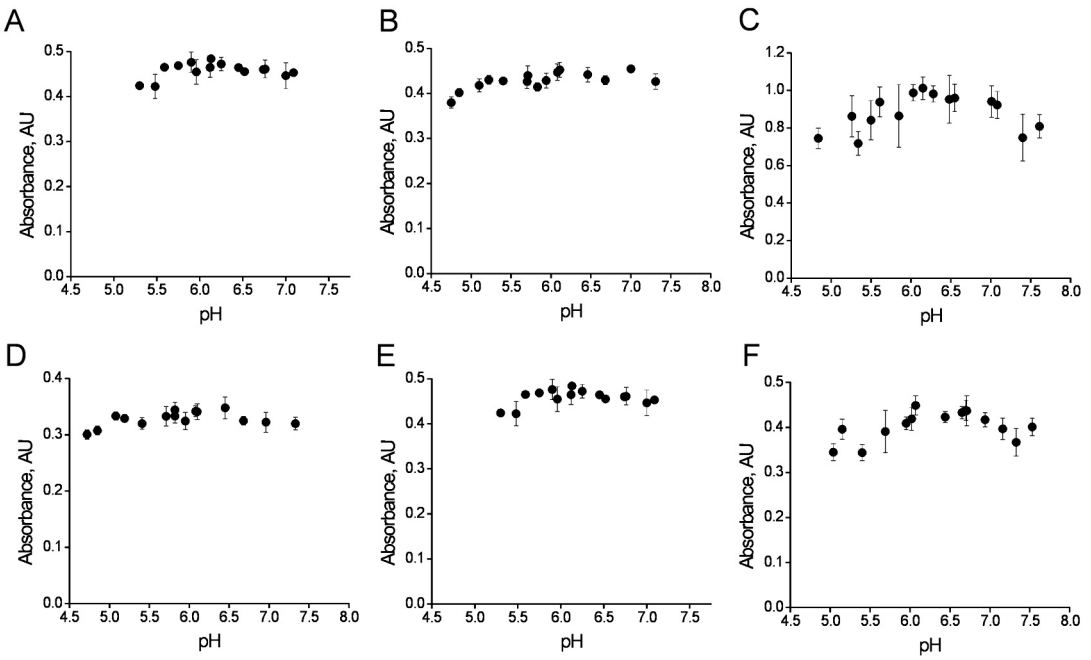

Fig. S4. MTS cell viability assay. The effect of pH and presence of peptide on cell viability were measured after each individual experiment for: (*A*) pHLIP in B104 cells (control), (*B*) pHLIP in COS-7 cells (control), (*C*) MβCD treatment+pHLIP in B104 cells, (*D*) MβCD+pHLIP in COS-7 cells, (*E*) P20G pHLIP in B104 cells (control) and (*F*) MβCD+P20G pHLIP in B104 cells. Graphed absorbance is shown at 490 nm and indicates metabolically active cells. Similar cell viability is observed across the studied pH range. The differences in relative absorbance between panels is caused by the different incubation times with the MTS reagent (1–4 h).

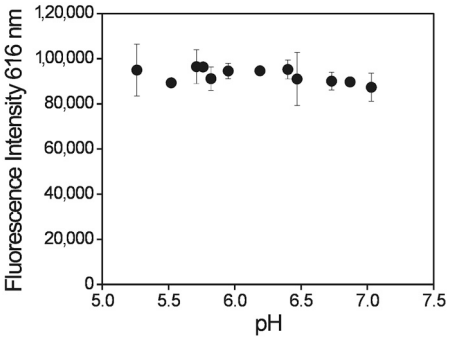

Fig. S5. pH has no effect on Alexa594 fluorescence. The fluorescence of Alexa594-labelled pHLIP at different pHs was measured. A similar intensity was observed across the studied pH range, indicating the probe fluorescence is not pH dependent in the studied range.

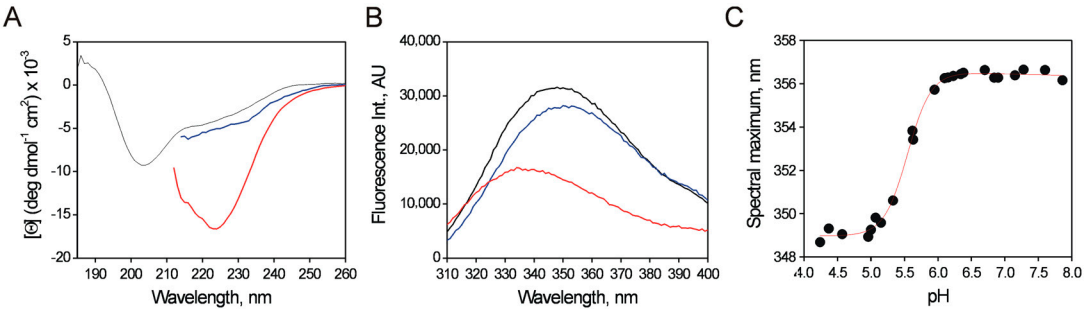

Fig. S6. Secondary structure, tryptophan environment and insertion pKa of pHLIP in liver total lipid extract. (*A*) CD experiments in buffer at pH 7.8 (state I; black lines) and liver extract liposomes at pH 7.8 (state II; blue lines) and pH 4.5 (state III; red lines). Large unilamellar vesicles were prepared using a Mini-Extruder. Peptide and lipid concentrations were 5 μM and 1.5 mM, respectively. Increased turbidity prevented data recording below 210 nm for samples containing liver lipids. (*B*) Emission fluorescence spectra in buffer at pH 7.8 (state I; black lines) and liver extract liposomes at pH 7.8 (state II; blue lines) and pH 4.5 (state III; red lines). Peptide and lipid concentrations were 1 μM and 0.4 mM, respectively. (*C*) The changes in fluorescence spectral center of mass were fitted to a sigmoidal fit, and the obtained pKa was 5.6–0.1.

Hydrophobic Thickness	Approx. AA # to span	Most Favorable Spanning Sequence Highlighted
21	14	GGEQNPIYWARYADWLFTTPLLLLDLALLVDADEGT
22.5	15	GGEQNPIYWARYADWLFTTPLLLLDLALLVDADEGT
24	16	GGEQNPIYWARYADWLFTTPLLLLDLALLVDADEGT
25.5	17	GGEQNPIYWARYADWLFTTPLLLLDLALLVDADEGT
27	18	GGEQNPIYWARYADWLFTTPLLLLDLALLVDADEGT
28.5	19	GGEQNPIYWARYADWLFTTPLLLLDLALLVDADEGT
30	20	GGEQNPIYWARYADWLFTTPLLLLDLALLVDADEGT
31.5	21	GGEQNPIYWARYADWLFTTPLLLLDLALLVDADEGT
33	22	GGEQNPIYWARYADWLFTTPLLLLDLALLVDADEGT
34.5	23	GGEQNPIYWARYADWLFTTPLLLLDLALLVDADEGT
37	24	GGEQNPIYWARYADWLFTTPLLLLDLALLVDADEGT
38.5	25	GGEQNPIYWARYADWLFTTPLLLLDLALLVDADEGT

Fig. S7. The length of the amino acid segment used to span each corresponding hydrophobic thickness was determined by calculating the spanning TM segment as a straight helix. The WT pHLIP sequence was scanned using the MPEx program developed by Stephen White's lab to determine the most hydrophobic segment of each length. These segments (highlighted yellow) were taken as the putative spanning segments for each hydrophobic thickness and the MPEx Totalizer was used to determine the per residue average hydrophobicity. The average values for the hydrophobic thicknesses of the lipids used in this study are plotted in Fig. 5*B*. The red residues in the pHLIP sequence denote the two spanning aspartic residues at positions 14 and 25.

A

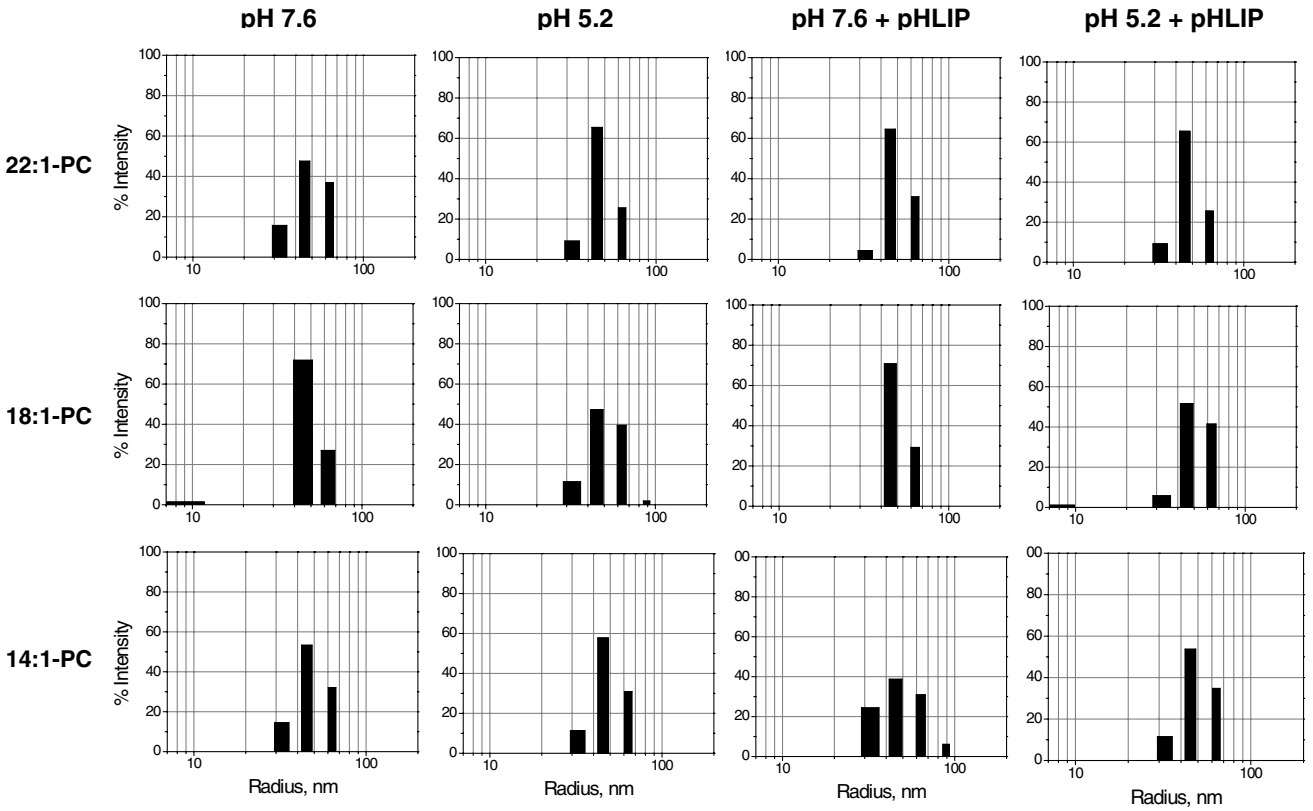

B

Mean hydrodynamic radius, nm

	pH 7.6	pH 5.2	pH 7.6 + pHLIP	pH 5.2 + pHLIP
14:1-PC	47.8±0.2	47.5±0.7	48.3±0.1	48.7±0.5
18:1-PC	48.1±1.3	49.1±0.1	48.8±0.2	49.0±0.5
22:1-PC	46.9±0.3	47.3±0.3	46.8±0.4	47.9±0.4

Fig. S8. LUV morphology characterization in different pH buffers and in the presence of pHLIP. Dynamic light scattering data of 14 : 1-PC, 18 : 1-PC and 22 : 1-PC LUVs were analyzed using two different approaches: (*A*) Regularization histogram were calculated by the nonnegative least square error algorithm. Particle hydrodynamic radii distribution is shown; (*B*) Monomodal analysis determination of the mean hydrodynamic radius, in nm. Average and Standard Deviation ($n = 3$ or 4) are shown. Experiments were performed in a DynaPro-801 TC (Protein Solutions) instrument at 25 deg. Lipid to peptide ratio was 200 to 1.

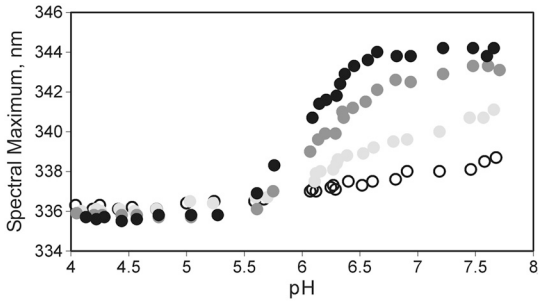

Fig. S9. pH-dependence of the fluorescence spectral maximum of WT pHLIP in 14:1-PC liposomes with different cholesterol content (white: 0%, light gray: 10%, dark gray: 20% and black: 30% cholesterol). Peptide concentration was 5 μM and lipid concentration 1.5 mM. Buffer concentration was 28 mM. Under these ionic strength conditions a cooperative transition was only observed in the presence of cholesterol, in contrast to the cooperative behavior observed for 14:1-PC liposomes at slightly lower ionic strength (Fig. 3*A*, *Inset*). This ionic strength dependency complicates any interpretation, and hence we decided to leave these data points out of our analysis.